
Distinguishing groundwater flow paths in different fractured-rock aquifers using groundwater chemistry: Dandenong Ranges, southeast Australia

S. O. Tweed · T. R. Weaver · I. Cartwright

Abstract Major ion geochemistry is used to qualitatively interpret groundwater residence times within an aquifer, and the extent of mixing between aquifers with distinctive mineralogy. In conjunction with hydraulic heads and stable isotope geochemistry, flow paths and inter-aquifer exchange are defined in a fractured-rock aquifer system in the Dandenong Ranges, southeast Australia. Stable isotopes indicate modern seasonal recharge throughout the system. At high elevations in the sub-catchment, which includes both marine Silurian-Devonian sedimentary and Tertiary basalt aquifers, Cl is derived primarily from cyclic salts, and differences in mineralogy result in groundwater from the basalt aquifer having higher TDS contents (123–262 mg/L) and (Ca+Mg)/Na ratios (0.9–1.3) than groundwater from the sedimentary aquifer (TDS: 55–79 mg/L; (Ca+Mg)/Na: 0.1–0.2). At low elevations, in areas of local groundwater discharge, the more regional flow system in the Silurian-Devonian sediments contains additional Cl from water–rock interaction and has distinctly higher TDS contents (517–537 mg/L). Differences in groundwater chemistry between the aquifers and between shallower and deeper flow systems highlights areas of inter-aquifer mixing. This is particularly important for aquifer vulnerability where groundwater quality in the deeper aquifer may be impacted by surface activities.

Résumé Les ions majeurs sont utilisés pour interpréter quantitativement les temps de résidence des eaux souterraines dans les aquifères, et l'étendue des zones de mélange entre les aquifères de différentes minéralogies.

Received: 18 July 2003 / Accepted: 17 April 2004

Published online: 4 June 2004

Springer-Verlag 2004

S. O. Tweed (✉) · T. R. Weaver

School of Earth Sciences,
University of Melbourne, 3010, Victoria,
Australia e-mail:
stweed@mail.earth.monash.edu.au Fax:
+61-3-99054903

I. Cartwright

School of Geosciences,
Monash University,
3800 Clayton, Australia

En regard de la répartition des charges hydrauliques et des informations données par les isotopes stables, les coulements et les échanges inter-aquifères sont définis dans un aquifère fracturé dans le Dandenong Ranges, SE de l'Australie. Les isotopes stables indiquent des recharges modernes et saisonnières travers le système aquifère. A haute altitude dans le sous-bassin versant, qui inclut des sédiments du Siluro-Devonien et des basaltes du Tertiaire, le chlore est d'abord driv des sels cycliques, et des différences minéralogiques dans les eaux souterraines sont observées selon l'aquifère : basalte tertiaire (TDS: 123–262 mg/L; Ca+Mg/Ca: 0.9–1.3) et sédiments primaires (TDS: 55–79 mg/L; Ca+Mg/Ca: 0.1–0.2). Aux basses altitudes, dans les zones locales de décharge des eaux souterraines, les coulements les plus régionaux possèdent des teneurs plus élevées en Chlore en provenance des interactions eau–roche, et des TDS plus élevés (515–537 mg/L). Des différences dans la chimie des eaux souterraines entre les aquifères et entre les systèmes d'écoulement de surface et les coulements profonds mettent en lumière les zones de mélange inter-aquifère. Ceci est particulièrement important pour la définition de la vulnérabilité ou la qualité des eaux souterraines en profondeur peuvent subir les impacts des activités de surface.

Resumen Se ha utilizado geoquímica de iones mayores para interpretar cualitativamente los tiempos de residencia del agua subterránea dentro de un acuífero, y el grado de mezcla entre acuíferos con mineralogía característica. De manera conjunta con presiones hidráulicas y geoquímica de isótopos estables, se han definido trayectorias de flujo e intercambio entre acuíferos en un sistema de acuífero de roca fracturada en las Sierras Dandenong, sureste de Australia. Los isótopos estables indican recarga estacional moderada a través del sistema. A elevaciones altas en la sub-cuenca que incluye acuíferos sedimentarios Silúrico-Devónicos y acuíferos basálticos Terciarios, el Cl se deriva principalmente de sales celicas. Las diferencias en mineralogía resultan en agua subterránea del acuífero basáltico que tiene mayores contenidos TDS (123–262 mg/L) y mayor relación $(Ca+Mg)/Na$ (0.9–1.3) que el agua subterránea de los acuíferos sedimentarios (TDS: 55–79 mg/L; $(Ca+Mg)/Na$: 0.1–0.2). A elevaciones bajas, en áreas de recarga local de agua subterránea, el sistema de flujo más regional en los sedimentos Silúrico-Devónicos contiene Cl adicional que se deriva de la interacción roca-agua y típico contenido TDS más alto (517–537 mg/L). Las diferencias en la química del agua subterránea entre los acuíferos y entre los sistemas de flujo más profundo y más somero resalta áreas de mezcla entre acuíferos. Esto es particularmente importante para la vulnerabilidad del acuífero donde la calidad del agua subterránea en el acuífero más profundo puede ser impactada por las actividades superficiales.

Keywords Hydrochemistry · Stable isotopes · Fractured rocks · CFCs · Australia

Introduction

Determining the processes that control groundwater chemistry is essential for effective water resource management and protection (e.g. Ho Jeong 2001; Edmunds et al. 2002). This is especially important in groundwater systems where the physical hydrogeology is complex due to fracture-hosted flow or the presence of multiple aquifers. In fractured-rock aquifer systems, understanding the distribution and rates of groundwater flow becomes difficult due to complex physical controls such as permeability contrasts between fractures and the surrounding rock matrix (Doughty and Karasaki 2002), and mapping fracture geometry and frequency. To manage groundwater resources in such flow systems, groundwater flow paths can be determined using multi-component geochemical tracers in conjunction with physical parameters. Where physical parameters are indicators of current flow, chemical compositions can reveal discrete groundwater flow paths.

In particular, non-conservative ions are effective tracers of flow paths since they record the reactions that occur as groundwater interacts with the host rock (e.g. Njitchoua et al. 1997; Huizar et al. 1998; Jankowski et al. 1998), compared to conservative tracers that largely indicate processes in the recharge areas (Edmunds and Smedley 2000). This paper expands on studies where different combinations of stable isotopes, major ions and trace elements have been used to define groundwater pathways, mixing and relative residence times (e.g. Weaver et al. 1995; Edmunds and Smedley 2000; Herczeg 2001; Lee and Krothe 2001; Swanson et al. 2001; Uliana and Sharp Jr. 2001).

This paper uses groundwater chemistry to determine groundwater flow paths as a qualitative measure of residence times in a fractured rock aquifer system. While TDS contents of groundwater increases with residence times, vertical and horizontal variations in TDS suggests mixing of groundwater from different aquifers and local recharge has occurred. These processes are constrained by reactive and conservative major ions, groundwater elevations, stable isotopes, and chlorofluorocarbons (CFCs). This research demonstrates that major ion geochemistry is a good discriminator of flow paths due to the distinct mineralogy of the different aquifers. The hydrochemical interpretations provide a model for improved management of groundwater resources and associated surface water in the study area, and is an approach which can be applied to other multiple aquifer and fractured rock systems.

Description of the Study Area

The study area is in the Dandenong Ranges sub-catchment, part of the greater Yarra Catchment, Victoria, Australia, as shown in Fig. 1. Previous investigations into water quality in the Yarra Catchment have concentrated primarily on its surface water (e.g. Port Phillip Catchment and Land Protection 1999). Earlier research into groundwater chemistry and flow in the Dandenong Ranges subcatchment highlighted the potential for the fractured rock system to be used as a water resource (Shugg 1996), and estimated that groundwater provides over 50% of the total flow to local rivers and streams (Shugg and O'Rourke 1995). Groundwater is used throughout the Yarra Catchment for domestic and agricultural practices, and is most intensively used for irrigation within the Dandenong Ranges sub-catchment (Port Phillip Catchment and Land Protection 1999).

The Yarra Catchment comprises unconfined fractured rock aquifers (Shugg 1996). Major aquifers in both the Yarra Catchment (Fig. 1) and the Dandenong Ranges subcatchment, as shown in Fig. 2a, include Silurian-Devonian marine

sediments, Devonian acidic volcanics, and Tertiary Older Volcanic basalts. Previous work by Shugg (1996) in the Dandenong Ranges sub-catchment, described groundwater flow via both weathered porous media and fractures in each of the major aquifers, with a degree of hydraulic continuity between them. Silurian-Devonian marine sediments, which form part of the Lachlan Fold Belt, underlie most of the Melbourne region and are extensive throughout the Yarra Catchment (Fig. 1) (Vandenberg 1988). Devonian rhyolitic extrusions and acid intrusives (Marsden 1988) form the highest elevations in the Yarra Catchment (Leonard 1992), for example Mount Dandenong in the southwest of the Dandenong Ranges subcatchment (Fig. 2a). Tertiary extrusive Older Volcanic alkali olivine basalts infill ancient stream valleys in the dissected Silurian-Devonian sediments. These basalts presently crop out as ridges in the Dandenong Ranges and in areas to the east and west of the sub-catchment (Fig. 1). The mineralogy of these aquifers is presented in Table 1. The rhyodacite mineralogy is based on the Ferny Creek rhyodacite (Marsden 1988), which is the dominant acid volcanic unit in the sub-catchment.

The type and depth of weathering in the Dandenong Ranges are highly variable. On the basalt-capped ridges, where infiltration of rainfall is rapid, the basalts are weathered to depths of 30–80 m, forming kaolinite by the following:

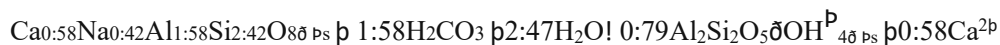
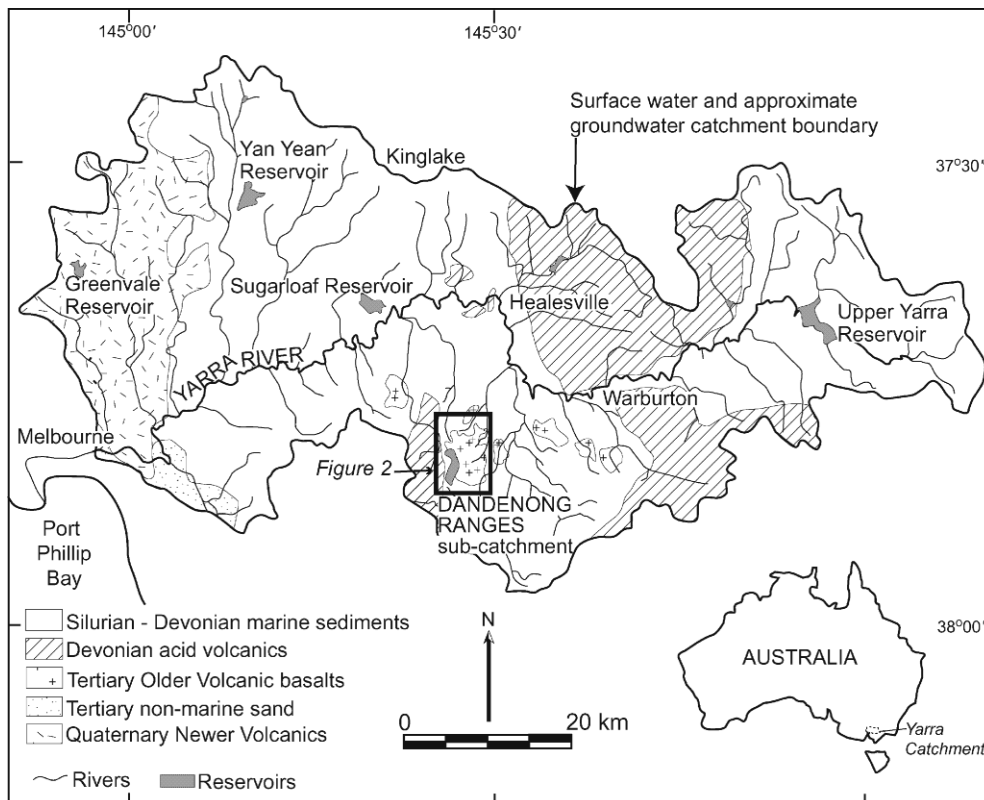


Fig. 1 Geology, reservoirs, streams, and location of the Dandenong Ranges sub-catchment within the Yarra Catchment (after Port Phillip Catchment and Land Protection 1999)

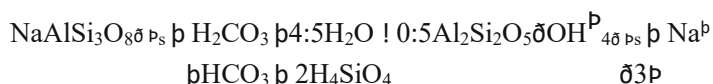


$\text{p}0:42\text{Na}^{\text{b}} \text{ p } 1:58\text{HCO}_3 \text{ p } 0:84\text{H}_4\text{SiO}_4 \quad \delta 1 \text{ p } \text{Shugg (1996) reported that montmorillonite is also present as the major fracture filling clay mineral in the basalt. This is formed from kaolinite (e.g. Stumm and Morgan 1996; Table 1) by the following:}$



$\delta 2 \text{ p}$

Weathering also occurs in the sediments, where kaolinite is produced from albite (e.g. Deer et al. 1992; Table 1) by the following equation:



Shugg (1996) also reported the presence of illite. Most natural samples of illite contain interstratified smectite (Deer et al. 1992): therefore it is likely that the illites indicated by Shugg (1996) also contain smectite layers.

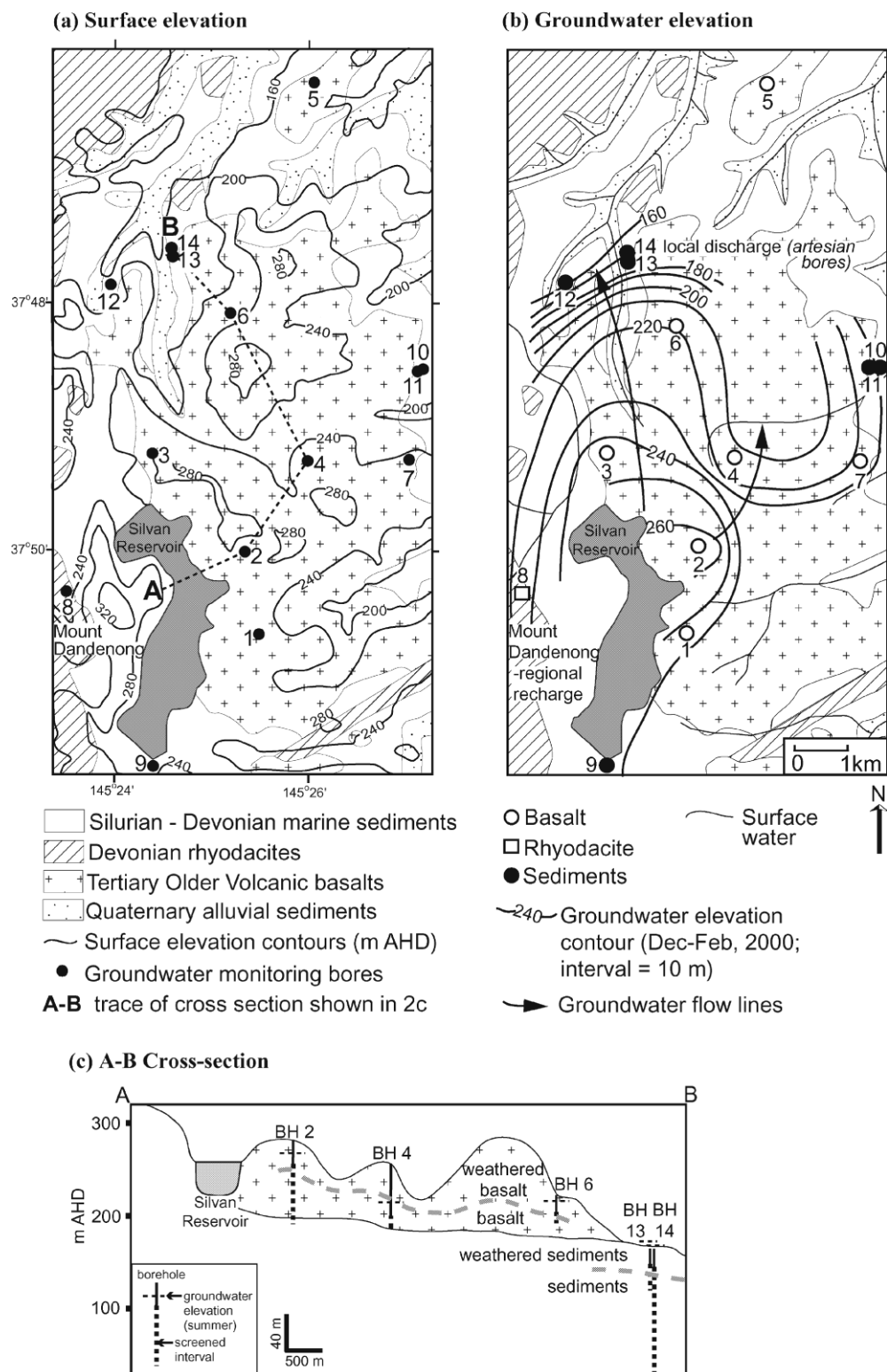
The climate in the Melbourne region is temperate with maximum rainfall during the Austral winter (Bureau of Meteorology 2002). In the Yarra Catchment, rainfall increases toward the northeast from ~600 to 1,400 mm year as the surface elevation rises from <250 to >1,000 m AHD (Australian Height Datum; Bureau of Meteorology 2000). The Yarra Catchment is part of the greater Port Phillip and Highlands basins (Victorian Resources Online 2003). In both basins, groundwater and surface water drain towards and discharge into the Port Phillip Bay (Fig. 1). Throughout the catchment, there is sufficient rainfall to support temperate rainforests, springs, and permanent streams fed from both runoff and baseflow (Shugg and O'Rourke 1995).

Within the Dandenong Ranges sub-catchment, rainfall levels also increase with surface elevations, for example average annual rainfall is 1,200 mm/year at Mt. Dandenong compared with 600 mm/year on the basalt capped ridges (Bureau of Meteorology 2000). Over distances of ~7 km, there are large topographic changes between the basalt-capped sediment ridges at 160–300 m and the rhyodacite hills at Mt. Dandenong (~600 m). Groundwater flow within this sub-catchment is towards the Yarra River. In areas of high groundwater elevations, large unsaturated zones indicate that streams recharge groundwater, whereas lower in the catchment there is evidence of groundwater recharging the streams in the local discharge area (Fig. 2b; Shugg 1996).

Sampling and Analysis

Groundwater samples were collected from 14 boreholes (BH) completed in the sediments, rhyodacite, and basalt (Table 2). Most boreholes in the basalt are located along ridges, whilst the boreholes in the sedimentary aquifer occur on the slopes (upper to mid slopes—BH 9–11; lower slopes—BH 12–14). Samples were collected from the middle of the screened intervals using a micro-purge (or low-flow) technique (e.g. Puls and Barcelona 1996) with a submersible pneumatic bladder pump. Ground-

Fig. 2 a Geology of the Dandenong Ranges sub-catchment (Melbourne Geology Map, 1:250000; Sheet SJ55-5), topography, and location of section (A-B). b Location of groundwater samples in the Dandenong Ranges distinguished by lithology. Generalised groundwater elevation (m AHD: Australian Height Datum) contours shown for summer (December through February) 2000. c Lithology, location and depth of boreholes along the cross-section A-B



water elevations were monitored whilst pumping to achieve minimal drawdown. BH 13 and 14 are flowing artesian bores, so samples from these bores were collected at the wellhead. Temperature, pH, Eh and electrical conductivity (EC) were monitored during pumping, or during flow for BH 13 and 14, using a flow-through cell. Groundwater samples were collected after these parameters stabilised.

Large screen intervals are not ideal for sampling groundwater, particularly in fractured rocks. In this study, groundwater sampled from BH 14 was from a slotted interval of 282 m (Table 2), and as discussed below, re-

Table 1 Dominant mineralogy and weathering products of different lithologies in the Dandenong Ranges sub-catchment

Sedimentary	Rhyodacites	Basalt
Major mineralogy		
Quartz ^a	Plagioclase (e.g. labradorite) ^c	Olivine (Fo ₇₃₋₈₀) ^d
Plagioclase (e.g. albite) ^b	Hypersthene ^c	Plagioclase (e.g. labradorite: An ₅₈₋₆₃) ^d
Biotite ^a	Biotite ^c	Pyroxene (e.g. salite) ^d
Muscovite ^a	Quartz ^c	
Weathering products		
Kaolinite ^b	Kaolinite ^b	Kaolinite ^b
	Montmorillonite ^b	Montmorillonite ^b
a		
Vandenberg (1988) ^b		
Shugg (1996) ^c		
Edwards (1956) ^d		
Price et al. (1988) (1988)		

sults are different between sample rounds. Further, it should also be recognised that the sample obtained will be from the area of highest flow along the screened interval (i.e. largest fracture conduit), even though chemical field parameters stabilise prior to sampling. This is a limitation when not using straddle-packers or short screen intervals, since samples from other hydraulic conditions may vary in chemical compositions (Shapiro 2002). For the purposes of this field-scale investigation, results are assumed to be approximate representations of groundwater interacting with the different aquifers.

Alkalinity, dissolved CO₂, and dissolved oxygen were measured in the field by titrations. Detection limits for alkalinity and dissolved CO₂ is <0.1 mg/L, and precision is approximately €10%. Detection limits for dissolved oxygen is <1 mg/L, and the precision is €1 mg/L. Samples for cation analyses were filtered (0.45 mm cellulose nitrate filter) and acidified to pH <2 (ultrapure 16 N HNO₃) in the field and analysed using a Perkin Elmer-Optima 3000 ICP-OES at Chemical Engineering Analytical Facility, University of Melbourne. Detection limits for cations is <1.0 mg/L, except for Si, which is <0.01 mg/L, and precision is approximately €10%. Unfiltered and unacidified samples for anions were analysed by ion chromatography at the Wairakei Research Centre, NZ. Detection limits for anions is <0.05 mg/L, except for Br which is <0.03 mg/L, and precision for these is approximately €5%. Ion charge balances for samples range between +8 and 16%.

Stable isotope (d¹³C and, d²H and d¹⁸O) ratios were analysed using the Finnigan MAT 252 mass spectrometer at Monash University, and the precision is d¹⁸O=€0.1‰; d²H=€1‰; d¹³C=€0.2‰. d¹⁸O values were measured via equilibration with CO₂ at 25C for 24–48 h, and d²H were measured via reaction with Cr (850C). Data were normalised following Coplen (1988) and d¹⁸O and d²H values are expressed relative to V-SMOW where d¹⁸O and d²H values of SLAP are 55.5 and 428‰ respectively. CO₂ from dissolved inorganic carbon (DIC) was liberated by acidification under vacuum in sealed sidearm vessels, and d¹³C values are expressed relative to PDB.

Groundwater samples were also collected for CFC-11, CFC-12 and ²²²Rn analysis in January, 2001. Samples for CFC analysis were collected using a N₂-pressurized bailer and flame sealed in a glass ampule. Samples from the two flowing artesian bores were collected directly from the wellhead after 1 h of flow and were also flame sealed in the field. Apparent CFC ages were calculated using an estimated recharge temperature of 18C, an elevation of 0 m, and pressure at 0.97 atm. Samples for ²²²Rn analysis were collected with a syringe from the pressurised bailer or wellhead and stored in bottles containing a mineral-oil base liquid scintillation solution. CFC and ²²²Rn analyses were performed at CSIRO Land and Water, Glen Osmond, South Australia.

Results and Discussion

Results of groundwater sampling during January 2000 (summer) are presented in Table 3. Results from just one sample round are presented as most groundwater samples showed reasonably low relative standard deviations (RSDs) of each major ion between sample rounds; RSDs were between 1 and 33% (median RSD: 7%). An exception to this is groundwater chemistry for BH 14. BH 14 has RSDs of major ions between 15 and 57% (median RSD: 39%). Since samples were collected at the wellhead, the changes in composition probably represent variations in flow from different depths of the large screened interval (282 m). This is discussed further below.

Groundwater Flow

Groundwater elevations roughly follow topography (Fig. 2b). Increased rainfall with elevation in the Dandenong Ranges sub-catchment (Bureau of Meteorology 2000) may imply that increased recharge in topographically higher areas is likely. However, other factors also affect groundwater elevations such as changes in aquifer characteristics (specific yield and porosity) and discharge rates (Healy and Cook 2002). Therefore, fluxes of recharge will vary between the different lithologies, and within the same lithology due to the complex fracture network.

and autumn (December to May) through to winter and spring (June to November), groundwater elevations increased by up to 6 m in all boreholes except BH 4. This increase reflects seasonal groundwater recharge as rainfall increases, and is explored further below using stable isotopes. In all aquifers groundwater hydrographs show a 2–3 mo lag time for autumn and winter rainfall to impact the groundwater elevations, although fluctuations are attenuated in some bores (Tweed 2003). During winter and spring, groundwater elevations increase by 21.4 m in BH 4. This is probably due to increased groundwater use for irrigation leading to large drawdowns over summer and autumn. These large seasonal variations in groundwater elevations at BH 4 results in hydraulic gradient reversals between groundwater and nearby surface water. During summer and autumn the creek recharges groundwater, whereas during winter and spring groundwater discharges to the creek.

In the sub-catchment, groundwater discharge also occurs approximately 5 km north of the basalt ridges where the surface elevation is ~165 m AHD (Fig. 2a). BH 13 and 14, completed in the discharge zone, are flowing artesian bores with groundwater elevations of ~171 and 170 m AHD respectively. The vertical hydraulic gradients between these bores are high (0.008–0.5 m/m; from middle to top of the screened intervals), resulting from the thinning of the basalt aquifer, high recharge rates and large variations in topography over relatively short distances (Fig. 2a). Effects of shallower and deeper flow systems on groundwater chemistry are discussed below.

Origin and Ages of Groundwater

As shown in Fig. 3, groundwater in the Dandenong Ranges sub-catchment originates as rainfall and has not been subjected to significant evaporation nor gas-water exchange. All $\delta^{18}\text{O}$ (6.5 to 5.5‰) and $\delta^2\text{H}$ (–41.8 to 32.2‰) values for groundwater plot on, or near, the local meteoric water line (Fig. 3), and are slightly lower than values for streams in the region ($\delta^{18}\text{O}$ = 5.9 to 5.1‰; $\delta^2\text{H}$ = 38.8 to 31.0‰).

Compared with $\delta^{18}\text{O}$ and $\delta^2\text{H}$ values of Melbourne precipitation, from the IAEA database (IAEA/WMO 1999), the isotopic ratios of groundwater and surface water are slightly lower than the median values of autumn (March to May) and winter (June to August) rainfall (IAEA/WMO 1999), and are significantly lower than spring (September to November) and summer (December to February) rainfall (Fig. 3). Lower isotopic values of groundwater compared with rainwater could result from altitude effects, and/or seasonal recharge of predominantly autumn and winter rainfall. The altitude effect results in lowering of both $\delta^{18}\text{O}$ (~0.15 to 0.5‰ per 100 m) and $\delta^2\text{H}$ (~1 to 4‰ per 100 m) values (Clark and Fritz 1997). Assuming an elevation difference of 0–600 m from Melbourne to Mount Dandenong, depleted isotopic values (from the Melbourne average) cover the range of groundwater and most surface water values (Fig. 3). The altitude affect is, therefore, a plausible explanation for depleted isotopic values in groundwater.

NA

Table 3 Chemistry of groundwater from the Dandenong Ranges, January 2000 (summer). NA sample contaminated, SI saturation index calculated using PHREEQC (Parkhurst and Appelo 1990)

Borehole number	Basalt		Rhodacite Sedimentary			
	a	34567	8 ^a	910	b	
DNRE bore number	983969839498408984079841498406983997993079928109769109770984099841198416					f
Groundwater elevation (m AHD)	241268244214169219224225243232229161171					170 ^f
Temperature (°C)	23.18151729252218241523211716					
pH	6.26.16.58.66.16.47.35.86.04.85.26.77.16.7					
EC (µS/cm)	18717021227732642965512086123141399768770					
TDS (mg/L)	1231191591802242624353556579242517537					
Eh (mV)	38628641037539233535532545074562774141					
Dissolved oxygen	448372871532<1<1					
mg/L						
Ca	(mg/L) 9.17.010.316.35.519.537.03.00.81.71.421.128.526.8					
Mg	(mg/L) 8.24.09.24.99.525.032.02.01.11.22.67.739.537.4					
Na	(mg/L) 15.016.017.035.543.327.056.016.08.019.020.141.057.854.5					
K	(mg/L) 2.4<1.02.31.51.31.94.02.0<1.00.80.63.51.61.8					
Si	(mg/L) as Si 24.37.426.06.638.823.418.68.13.33.95.014.214.925.6					
SO ₄	(mg/L) 2.55.53.54.71.52.76.0<0.11.71.93.41.5<0.1<0.1					
Cl	(mg/L) 22.020.732.040.057.059.0103.922.112.232.036.053.0102.0118.0					
Br	(mg/L) 0.11<0.030.120.170.220.220.28<0.030.080.110.180.200.340.36					
HCO ₃	(mg/L) 3951587066103177101641099253230					
CO ₂	mg/L -989249-95-12991170168106250220					
CFC-11 average	pg/kg ^e -<2527<25-22136--<25<25<25-					
CFC-11 date recharged ^e	CFC-11 date					
CFC-12 average	pg/kg ^e -<1966<2037<1592<1641<2061<20961<1961<1961					
CFC-12 date recharged ^e	CFC-12 date					
²²² Rn (Bq/L) ^e	-<1966<185<142<1990.5<1613<19563<1986<2161					
d ¹³ C‰ V-PDB	^d -12.9-16.8-19.6-17.9-15.6-17.3-15.8-18.5-19.9-18.0-18.9					
d ¹⁸ O‰ V-SMOW	-6.2-6.5-6.3-6.0-6.0-6.2-6.0-5.8-6.1-6.2-6.3-6.4-6.0-6.2					
d ² H‰ V-SMOW	-39.6-41.4-39.1-35.7-36.2-38.9-36.7-35.9-38.2-37.6-38.1-40.0-36.1-37.2					
SI Calcite	-3.32-2.55-0.15-2.34-4.18-4.51-6.22-5.64-1.87-0.92-1.49					
SI SiO ₂	(a) -0.64-1.16-0.61-1.23-0.44-0.66-0.76-1.03-1.55-1.48-1.33-0.87-0.85-0.62					

^a Results for January 2001

^b Results for May 2000

^c Eh corrected for standard hydrogen electrode (Stumm and Morgan 1996)

^d Results for October 2001

^e Results for February 2001

^f Measurements from Shugg (1996) during summer 1991

Table 4 Seasonal differences in groundwater elevation showing higher levels during winter/spring (June to November) and lower levels in summer/autumn (December to May)

Borehole number	Basalt/Rhyodacite/Sedimentary	
	Basalt/Rhyodacite	Sedimentary
1234567891011121314		
DNRE bore number 983969839498408984079841498406983997993079928109769109770984099841198416		
Groundwater elevation (mAHD)		
Winter 1999 (July)	241.2-244.3	225.3170-5220.6226.6225.5-235.2231.2161.0--
Spring 2001 (October)	269.6243.6234.9-221.2-225.5243.2235.5231.9161.6--	
Summer 2000 (January)	240.7-243.9213.5168.7219.1223.7-243.2-229.3161.0171.0168.0	
Autumn 2000 (May)	263.6243.3225.7-219.9--232.3-160.4--	
Summer 2001 (January)	267.9243.1214.9168.1218.5-224.9243.0233.8229.9161.2--	
Maximum difference between winter/spring and summer/autumn (m)		
	0.55.91.221.42.52.72.90.60.23.22.50.6--	

However, there is also evidence of seasonal recharge to the groundwater system. In this temperate climate, rainfall at Mt. Dandenong is greater during winter months (median values: 80–117 mm/mo) compared with summer (median values: 40–88 mm/mo; Bureau of Meteorology 2002). Higher groundwater elevations during winter and spring (Table 4) imply seasonal recharge. Thus, in addition to an altitude affect, increased recharge from cooler rainfall will result in the groundwater having lower isotopic values than those of average Melbourne rainfall. The similarities in stable isotope ratios of groundwater from the sedimentary, rhyodacite and basalt aquifers indicate that all groundwater in the Dandenong Ranges subcatchment was recharged under similar conditions reflecting the current climate.

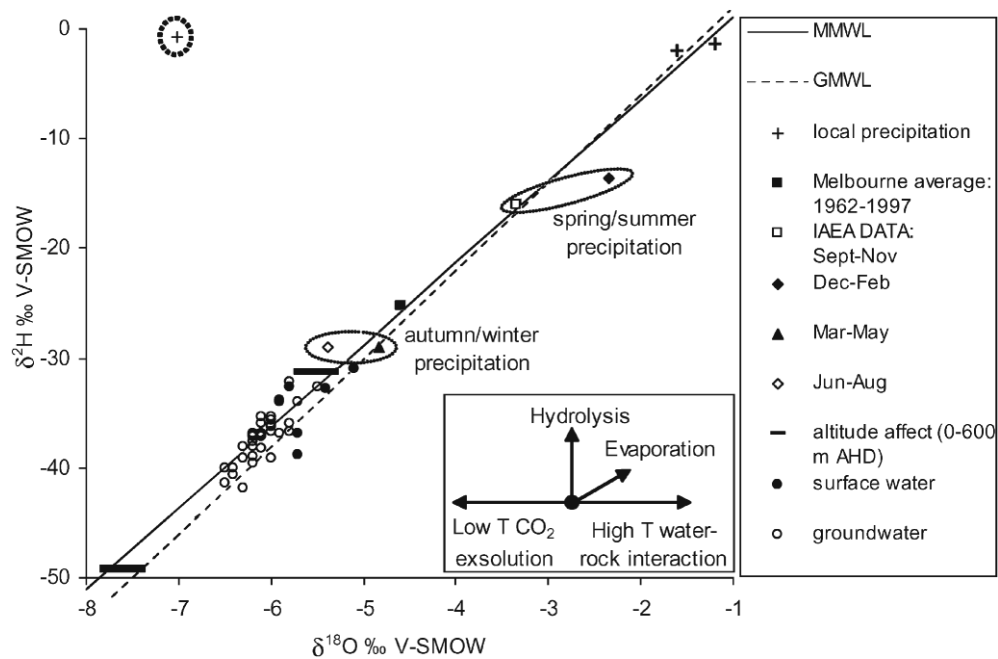
The lower isotope ratios of surface water compared with rainwater (Fig. 3) can be explained through the combined affects of groundwater providing >50% of the total flow, and the altitude affect. The slightly higher surface water $d^{18}O$ and d^2H values compared with groundwater may indicate some evaporation (although there is little shift from the MWLs), and/or less-selective rainfall input from streams receiving surface runoff throughout the year.

Apparent ages (Plummer and Busenberg 1999) of ground-water in the Dandenong Ranges were estimated using CFC-11 (trichlorofluoromethane ($CFCl_3$) atmospheric lifetime: 45±7 years) and CFC-12 (dichlorodifluoromethane (CF_2Cl_2) atmospheric lifetime: 87±17 years). Since the porosity of the basalt, rhyodacites and sediments will differ within and between the different aquifers, penetration of CFCs with depth will also vary. Therefore, limitations of CFC dating in this groundwater system is that the ages do not necessarily equate to groundwater residence times, as they will also be affected by the vertical velocity, aqueous and gaseous diffusion coefficients, water table fluctuations, and connectivity of fracture apertures (Plummer and Busenberg 1999).

CFC-11 and CFC-12 ages are distinctly different (Table 3), except for groundwater in BH 6. When compared to CFC-11 and -12 concentrations in equilibrium with the atmosphere, most values indicate that there has either been (a) loss of CFC-11, or (b) preferential addition of CFC-12 (Fig. 4a). Loss of CFC-11 can occur during microbial degradation in anaerobic environments (Plummer and Busenberg 1999). However, this is unlikely in the Dandenong Ranges since groundwater in most areas contains dissolved oxygen (Table 3). Enrichment of CFC12 can occur during dissolution of air bubbles that are trapped during recharge via fractures or turbulent flow. This excess air results in CFC-12 enrichment, because CFC-12 has a lower solubility compared with CFC-11 (Cook et al. 2003). Applying this to the fractured rock system of the Dandenong Ranges implies that groundwater was recharged over 40 years ago in the basalt and sedimentary aquifer, except for groundwater at BH 6.

The greater enrichment of CFC-12 in groundwater from the sedimentary aquifer (Fig. 4a) may indicate increased fracture vs. matrix flow in this aquifer compared

Fig. 3 Stable isotope ratios for local precipitation (July and August, 1999), surface water and groundwater (July and August, 1999, and January 2000) relative to the Melbourne meteoric water line (MMWL; Cheng 1998) and global meteoric water line (GMWL; Craig 1961). The local precipitation value circled is typical of the first rain from water vapour evaporated from seawater at low humidity (50%; e.g. Clark and Fritz 1997). IAEA data points (IAEA/ WMO 1999) are median values of precipitation at the Melbourne station (1995–1997) for the months December to February, March to May, June to August, and September to November, and the average for Melbourne over the years 1962–1997. The range of values from the altitude affect (from 0 to 600 m AHD) is shown, and was calculated using the Melbourne average



data point (Clark and Fritz 1997)

with the basalt, thereby resulting in greater turbulence during recharge. This area of the sedimentary aquifer, BH 10–11, also has anomalously high ^{222}Rn concentrations compared to all other samples (Fig. 4b), which may also be due to increased fracture flow. Factors which can result in ^{222}Rn variations include heterogeneities in distribution and aquifer porosity close to parent nuclides (uranium and

226

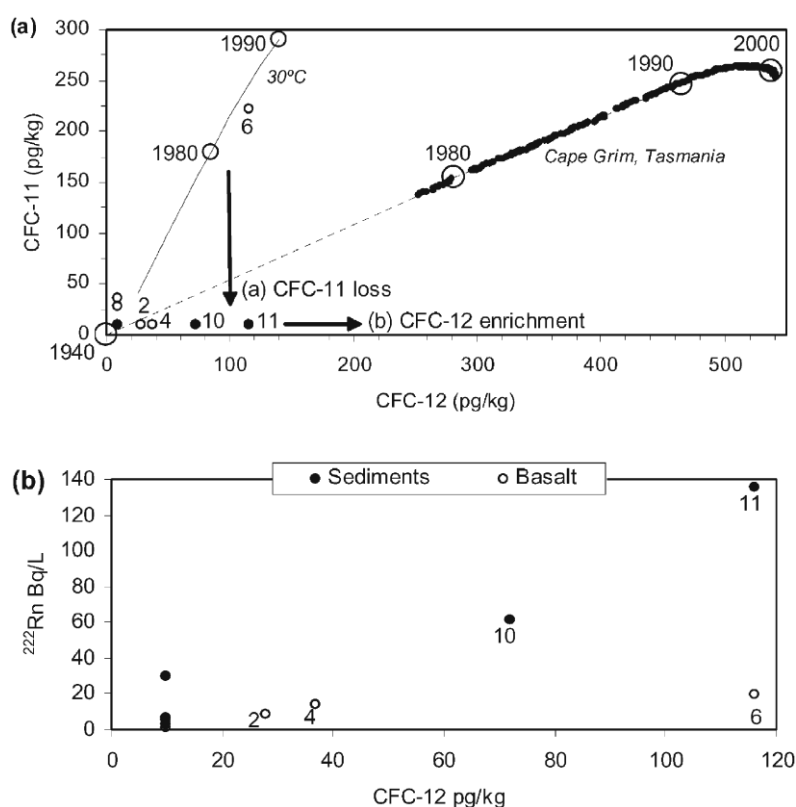
Ra), and groundwater residence time (e.g. Folger et al. 1997; Cook et al. 1999). In fractured rock systems, the measured ^{222}Rn concentrations are commonly higher on fracture surfaces compared to the matrix. There is still decay of ^{226}Ra to ^{222}Rn in the matrix, however transport of ^{222}Rn in small pores in the matrix will only be released by diffusion, compared to advective flow in fractures or larger pores (Cecil and Green 1999). Higher ^{222}Rn concentrations may also result from the greater concentrations of uranium in sediments (e.g. 2–9 ppm; Bierlein et al. 1999) compared with basalt (e.g. 0.4–1.2 ppm; Martin and McCulloch 1999). The small number of data points limits investigation into the extent fracture flow affects

^{222}Rn concentrations.

For groundwater in the basalt aquifer young enough to be dated (BH 6) the estimated recharge date is 1976–1979. Compared to other areas of the sub-catchment, the water table in the basalt ridges at BH 6 is relatively shallow (depth to water ~5 m, other bores ~10–44 m). This would reduce travel times, interaction with excess air, and possibly the extent of fracture flow in the weathered profile. The decreased importance of fracture flow in this area is also indicated by the low ^{222}Rn concentrations in groundwater from this bore (Fig. 4b). In addition to less fractures, reduced travel times for recharge via the thinner unsaturated zone at BH 6 would also result in a more representative apparent CFC age. Cook and Solomon (1995) found that increased unsaturated zones result in greater lag times for CFC dates (up to 15 years in a 30 m unsaturated zone). At BH 6, rapid recharge of rainfall is also evident from bore and stream hydrograph data collected by Shugg (1996) that show that groundwater and stream levels are in phase.

Compared to the curve of CFC-11 and -12 values at Tasmania (Fig. 4a), groundwater at BH 6 was probably recharged during warmer conditions. The groundwater CFC values are more similar to estimated values in equilibrium with the atmosphere at 30°C (after Cook et al. 2003), although this temperature is higher than the estimated groundwater temperature. When compared to these values in equilibrium with the warmer atmosphere, CFC-11 and -12 values of groundwater at BH 6 results in a more recent recharge estimate (~1984) than the apparent CFC age calculated used 18°C (1976–1979). Recharge dates at BH 6 will be more recent than the calculated CFC age because of mixing with older groundwater. The CFC age therefore represents mixing between groundwater through-flow and modern recharge. In order to compare the CFC age of groundwater at BH 6 to transit times in the basalt aquifer, between BHs 2 and 6 (Fig. 2c), the average linear velocity was calculated. These calculations assumed only horizontal flow in the basalt aquifer, a hydraulic conductivity value of 0.3 m/day (Shugg 1996), and an estimated porosity value of 20% (Domenico and Schwartz 1998). The transit time is ~460 years; over 16 times the CFC age at BH 6. This result indicates that modern recharge is likely to be mixing with through-flow and is supported by the major ion chemistry (discussed below). Quantitative assessment of groundwater residence times would therefore require additional dating using techniques such as radiocarbon. However, in this study, evolution of these groundwaters including flow downgradient and the vertical gradation from a local to a regional system are qualitatively explored using groundwater chemistry.

Fig. 4 a CFC-11 and CFC-12 values for groundwater sampled relative to values in equilibrium with the atmosphere at Cape Grim, Tasmania (41S, 145E; 1978–2003; Cunbold et al. 1994; Hartley et al. 1996; Cunbold et al. 1997). Most samples show either the effects of CFC12 enrichment or CFC-11 loss. Concentrations for CFC-12 < 20 and CFC-11 < 25 are below detection limits. Close to BH 6 are approximate CFC-11 and CFC12 values in equilibrium with the atmosphere at 3°C (solid line; after Cook et al. 2003). b High ^{222}Rn concentrations are observed in groundwater from the sediments where CFC-12 enrichment is also high



Groundwater Chemistry

As shown in Fig. 5, TDS values generally increase from 123 to 537 mg/L with decreasing groundwater elevations between the recharge and discharge areas. In general, pH increases with increasing TDS contents, reflecting increasing water–rock interactions along groundwater flow paths, which are discussed further below. Low pH values (4.8–5.2) in groundwater from some areas of the sedimentary aquifer (Table 3) may result from minor pyrite oxidation occurring during infiltration of rainfall, since pyrite is present in the sediments (Vandenberg 1988). These samples have dissolved oxygen (3–5 mg/L), whereas further along the flow path and at lower elevations in the sediments dissolved oxygen is absent and pH values are higher (6.7–7.1; Table 3).

Total dissolved inorganic carbon concentrations increase from 2.3–4.0 mmol/L in areas of high groundwater elevations in the basalt and sedimentary aquifers (BH 2–3 and 9–11), to 8.8–9.8 mmol/L in the discharge area (BH 13, 14). The sources of this carbon may include marine carbonate in the sedimentary aquifer, secondary calcite present in fracture fillings (Sanders 1992), and soil zone CO_2 . Groundwater in the discharge area is closer to being saturated with respect to calcite than other samples (Table 3). However, $\delta^{13}\text{C}$ values in groundwater, ranging from 19.9 to 12.9‰ V-

PDB (Table 3), indicate that soil zone CO_2 is the dominant source of inorganic carbon. Major vegetation in the sub-catchment includes eucalypt forest, pasture, market flowers, fruits and vegetables. These are C3 plants (no C4-producing crops present) that have $\delta^{13}\text{C}$ values between 24 and 30‰ V-PDB, and soil CO_2 with $\delta^{13}\text{C}$ values of approximately 23‰ VPDB (Clark and Fritz 1997). $\delta^{13}\text{C}$ values do not increase with increasing TDS contents, and therefore are not from progressive carbonate dissolution along flow paths. Instead, increasing total inorganic carbon with increasing TDS results from soil zone input. This implies recharge occurs across the catchment, there is a continuous supply of soil CO_2 driving weathering reactions (Clark and Fritz 1997), and illustrates the vulnerability of the system to surface contaminants.

As shown in Fig. 6, weathering reactions of groundwater interaction with the different aquifers results in distinctive major ion ratios. All samples have low SO_4 concentrations (<0.1–6.0 mg/L) and relatively high silica concentrations (3.3–38.8 mg/L Si; Table 3). Within the

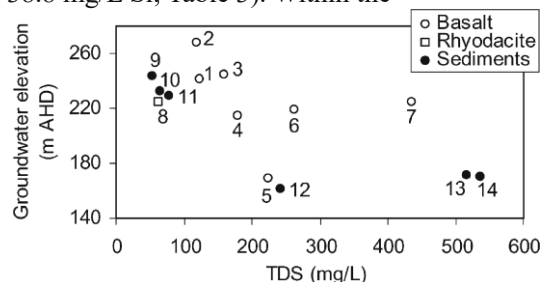


Fig. 5 Variations in TDS content both vertically and horizontally within the basalt and sedimentary aquifers

pH range, Si will most likely be present as $\text{H}_4\text{SiO}_4^\circ$, rather than H_3SiO_4 or $\text{H}_2\text{SiO}_4^{2-}$ (Langmuir 1997). Groundwater in the basalt aquifer is characterized by more variable $\text{H}_4\text{SiO}_4 + \text{HCO}_3$ concentrations relative to Cl, compared to more variable $\text{Cl} + \text{HCO}_3$ concentrations relative to H_4SiO_4 in groundwater from the sedimentary aquifer (Fig. 6). Increasing concentrations of HCO_3 relative to $\text{Cl} + \text{H}_4\text{SiO}_4$ in groundwater in the sedimentary aquifer corresponds with increasing TDS contents (65–517 mg/L). Figure 6 also illustrates the large variation in Na, Mg and Ca. Groundwater in the sedimentary aquifer changes from Na to Na–Mg–Ca type with increasing TDS. Groundwater from the basalt aquifer has varying ratios of Na–Mg–Ca that do not correlate with TDS. Groundwater from the rhyodacite aquifer is dominated by Cl –Na– H_4SiO_4 and is distinct from that in both the basalt and sedimentary aquifers (Fig. 6). As discussed below, these differences in the dominant species in groundwater from the different aquifers are the product of water–rock interaction and mixing.

Groundwater chemistry in the basalt aquifer

For groundwater in the basalt aquifer (BH 1–7), rapid recharge of rainfall and high topographic drive results in potentially short residence times. As there is limited opportunity for water–rock interaction, TDS contents are low and cyclic salts will be the major source of Na and Cl in the groundwater. Cl/Br and Na/Cl ratios can constrain sources of Na and Cl (e.g. Davis et al. 2001; Vengosh and Hendry 2001). As shown in Fig. 7, groundwater samples from the basalt aquifer show an increase in molar Cl/Br ratios (450–840) with increasing TDS contents, whereas molar Na/Cl ratios vary with increasing TDS.

Groundwater with TDS contents <300 mg/L in the basalt aquifer has Cl/Br ratios that are likely to result from variations in the cyclic input (Fig. 7a). Cl/Br ratios are lower than seawater values (650–660) and fall above the range in precipitation near coastlines (290–400) (Davis et al. 1998). Whereas groundwater with higher TDS contents (BH 7) indicates an additional Cl source, potentially from mixing with more saline groundwater in the sedimentary aquifer since this bore is screened at the interface of the two aquifers (Table 2). The Na/Cl ratios are also similar to more saline groundwater in the sedimentary aquifer (Fig. 7b), further supporting mixing at this interface.

By comparison with Cl/Br ratios, the greater range of Na/Cl ratios in groundwater with TDS contents <300 mg/L indicates affects of water–rock interaction (Fig. 7b). The deeply-weathered profiles (30–80 m) and the presence of kaolinite and montmorillonite in the basalt aquifer (Shugg 1996) indicate that water–rock interaction has occurred. Where groundwater in the basalt aquifer has higher Na/Cl ratios than typical rainfall values of 0.8 (Langmuir 1997), this suggests some Na is derived from water–rock interaction, e.g. plagioclase dissolution (re-

Fig. 6 Relative concentrations of dominant species illustrating large variations in groundwater chemistry from sedimentary vs. basalt aquifers. With increasing TDS, groundwater from the sedimentary aquifer has increasing HCO_3^- relative to Cl and H_4SiO_4 , and increasing Ca and Mg relative to Na. Groundwater from the basalt aquifer shows large variations in H_4SiO_4 concentrations relative to HCO_3^- and Cl, and changing (Ca+Mg)/Na ratios, regardless of the TDS. Groundwater from the rhyodacites has a distinct HCO_3^- –Cl– H_4SiO_4 composition. The circled samples from the basalt aquifer are subject to mixing with groundwater from the sedimentary aquifer

action 1) or exchange with Ca (Fig. 7b). Dissolution of plagioclase present in the basalt could also result in the observed increasing HCO_3^- concentrations with increasing pH (consumption of CO_2 ; e.g. reaction 1). The plagioclase is

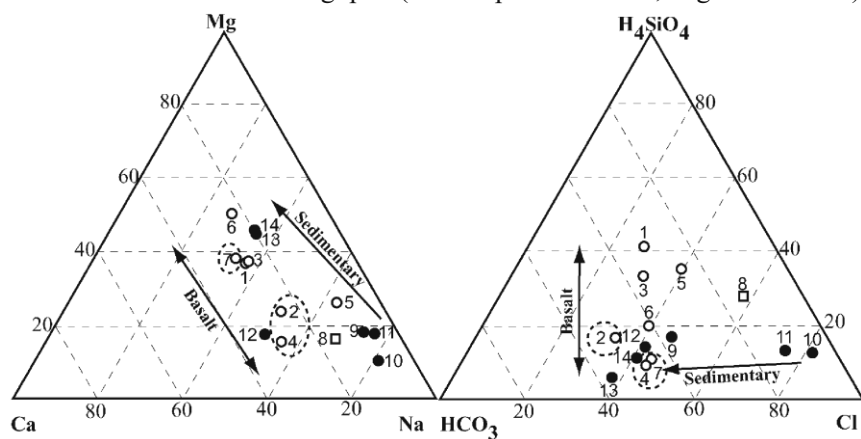
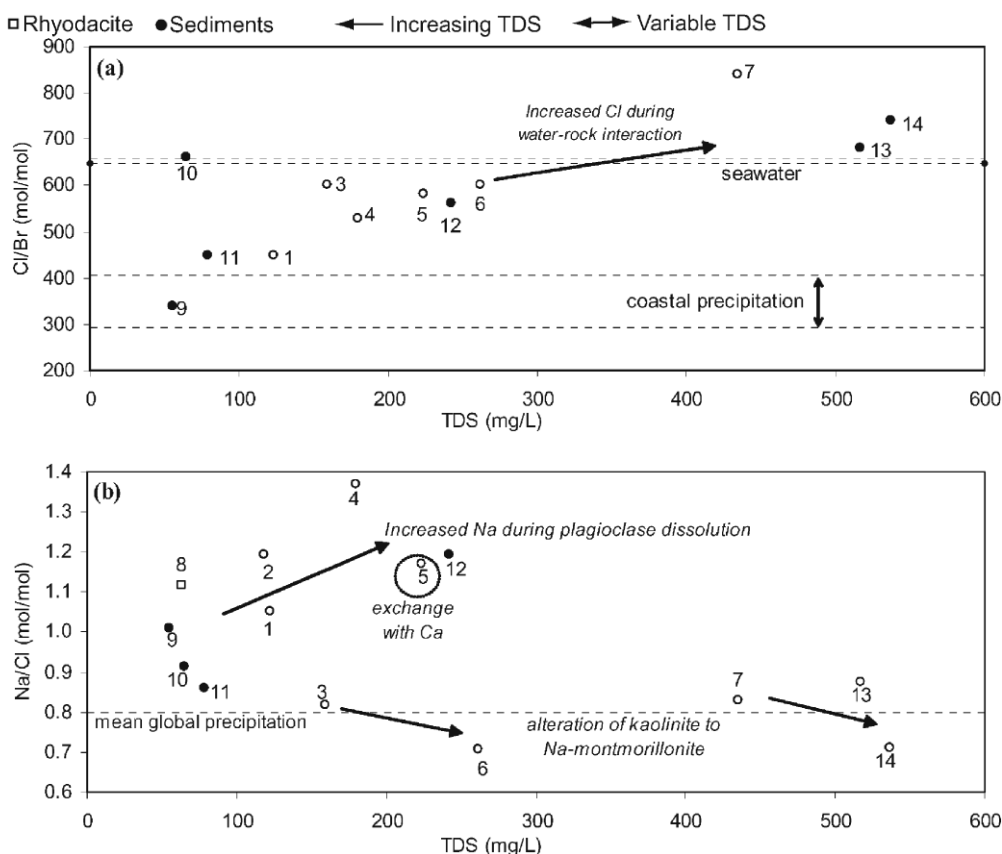


Fig. 7 a Cl/Br and b Na/Cl ratios indicating processes affecting Na and Cl concentrations in groundwater from the Dandenong Ranges (symbols as for Fig. 6) relative to Cl/Br ratios for seawater and coastal precipitation (Davis et al. 1998), and relative to Na/Cl ratios for mean global precipitation (Langmuir 1997). Ratios indicate a general increase in Cl with respect to Na and Br as water–rock interaction increases (e.g. increasing TDS)



labradoritic and this is reflected in the greater Ca/Na ratios compared groundwater interacting with the sediment mineralogy, as shown in Fig. 8a. Alternatively, the lower Na/Cl ratios than rainfall values (Fig. 7b) could result from alteration of kaolinite to Na-montmorillonite (reaction 2; Stumm and Morgan 1996). The presence of these clays in the

basalt aquifer (Shugg 1996) can also result in groundwater with very low Ca/Na ratios (e.g. BH 5; Fig. 8a), due to ion exchange (e.g. Jankowski et al. 1998) on the high cation exchange capacity surfaces of montmorillonite clays (CEC: 80–150 meq/100 g; Langmuir 1997).

Additional major weathering reactions in the basalt aquifer include dissolution of the abundant Mg-rich (Fo_{73–80}) olivine (e.g. Faust and Aly 1981) by the following equation:



04p

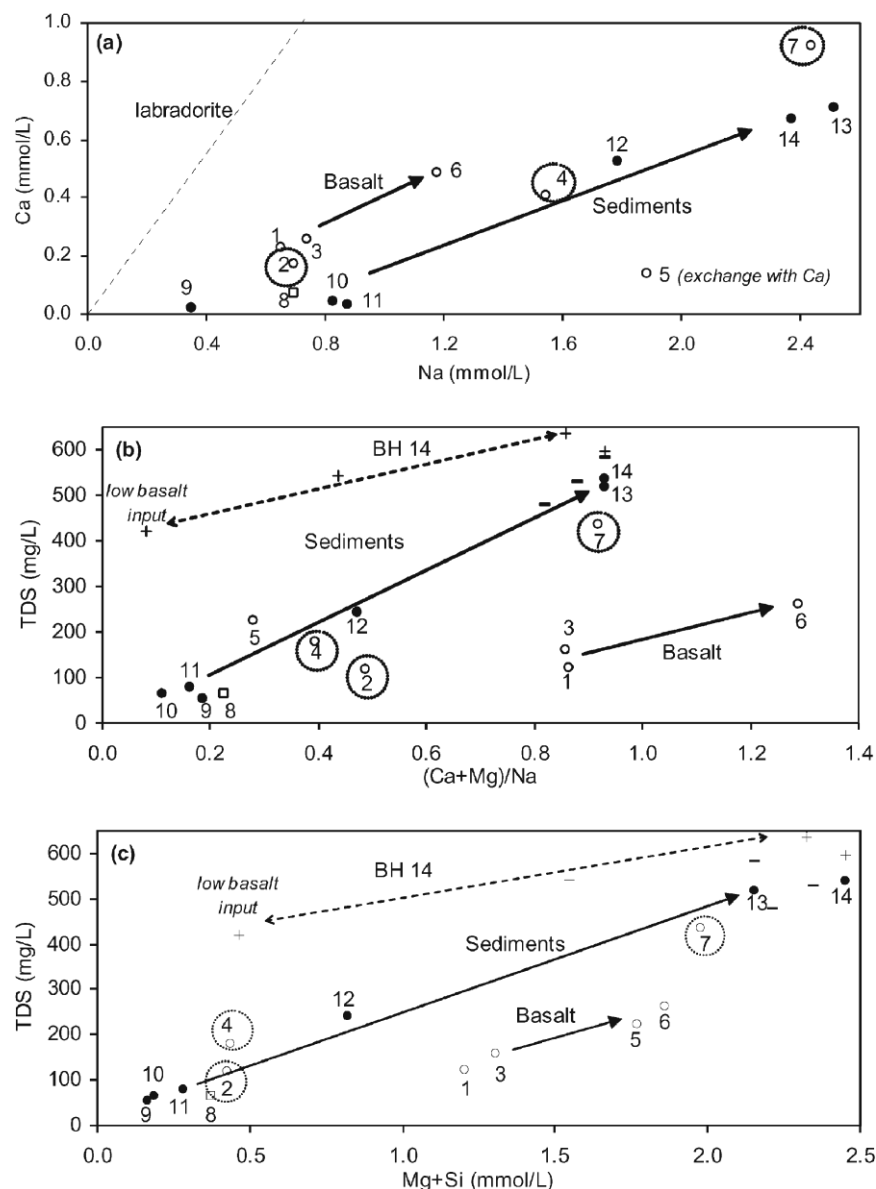
with analogous reactions for fayalite. These weathering reactions produce groundwater with a chemical composition that is clearly distinguishable from that of the sedimentary aquifer. TDS contents increase along flow paths primarily due to olivine and plagioclase dissolution. Groundwater from BH 5 has a lower (Ca+Mg)/Na ratio (Fig. 8b) due to Na and Ca exchange, but has Mg and Si concentrations that are typical of groundwater samples from the basalt aquifer (Fig. 8c). Therefore, groundwater primarily interacting with the basalt aquifer can be characterised by the increasing Mg, Si and Ca relative to Na as water–rock interaction increases (from BH 1, 3–6; Fig. 8). This implies that groundwater at BH 6 has a major through-flow component from the basalt aquifer, even though groundwater in this down-gradient area can be dated using CFCs. Groundwater in the basalt is therefore recharged across the catchment, resulting in relatively short net residence times.

Variations from these geochemical trends in the basalt aquifer highlight areas where mixing with deeper groundwater occurs. Low Ca/Na ratios, (Ca+Mg)/Na ratios, and Mg+Si concentrations (circled in Fig. 8) in groundwater from the basalt aquifer results from mixing with groundwater from the sedimentary aquifer. Mixing occurs in bores where the screen interval intersects the basalt-sediment contact (BHs 2 and 7), and where the screened interval extends to ~5 m above the sedimentary aquifer and is impacted by local pumping (BH 4) (Table 4).

Groundwater Chemistry in the Rhyodacite Aquifer

The low TDS (63 mg/L) and proximity to elevated topography (Fig. 2a) indicate that groundwater in the rhyodacite aquifer is largely influenced by local recharge. Water–rock interaction predominantly involves dissolu-

Fig. 8 Distinct groundwater composition in the basalt and sedimentary aquifers (symbols as for Fig. 6). a Groundwater interacting with the basalt aquifer, and therefore dissolution of labradorite, has higher Ca/Na ratios compared to groundwater interacting with the sedimentary aquifer (albite dissolution). Circled samples are bores screened in the basalt aquifer but compositionally indicate mixing with groundwater from the sedimentary aquifer. b Increased $(\text{Ca}+\text{Mg})/\text{Na}$ relative to TDS in the basalt aquifer results from labradorite and olivine dissolution. The lower $(\text{Ca}+\text{Mg})/\text{Na}$ ratio in groundwater from the basalt aquifer at BH 5 is due to exchange of Ca with Na-clay. Also shown are the results of different sampling rounds from BH 13 (–) and 14 (+). c Relative to TDS, high concentrations of Si and Mg in groundwater from the basalt aquifer compared to those in groundwater from the sedimentary aquifer indicate that high silica concentrations in groundwater are not just a function of residence time



tion of plagioclase to produce kaolinite (reaction 1), as indicated by the slightly elevated Na/Cl ratio (1.1) compared with rainfall (Fig. 7b), and relatively low $(\text{Ca}+\text{Mg})/\text{Na}$ ratio (Fig. 8b). The Ca/Na ratio is lower than expected from labradorite dissolution (Fig. 8a), indicating either dissolution of a more Na-rich plagioclase, or subsequent ion exchange of Ca with Na. Identifying the input of groundwater from this rhyodacite aquifer into the sedimentary or basalt aquifers is difficult because major ion composition is characterised using only one sample. However, relative major ion concentrations in Fig. 6 show a distinctive $\text{HCO}_3\text{--H}_4\text{SiO}_4\text{--Cl}$ ratio, unlike other groundwater samples from the basalt and sedimentary aquifers.

Groundwater chemistry in the sedimentary aquifer Groundwater from the sedimentary aquifer has distinctly different major ion composition (e.g. Fig. 6) and a larger range of TDS contents than groundwater interacting with the basalt (Fig. 5). Also, compared to groundwater from the basalt aquifer, increasing TDS contents (Fig. 5) and changes in major ion chemistry (Fig. 6) more clearly reflect the position of groundwater along the flow path.

At high groundwater elevations in the sedimentary aquifer, >220 m AHD, lower TDS contents are associated with large variations in Cl/Br ratios (340–660) that represent variations in the input from a cyclic source (Fig. 7a). Elevated Na/Cl ratios (0.9–1.0) (Fig. 7b), and the presence of kaolinite (Shugg 1996) suggest incongruent albite dissolution (reaction 3) during water–rock interaction. Similar to groundwater in the basalt aquifer, there is a continuous supply of soil zone CO_2 in the sedimentary aquifer to drive weathering reactions (Table 3).

Compared to groundwater at high elevations in the basalt aquifer, groundwater interacting with the relatively quartz-rich matrix of the sediments has lower TDS contents (Fig. 5). Therefore, differences in mineral solubility limits comparison of relative residence times between these two aquifers, but enables inter-aquifer mixing to be constrained. Lower Ca/Na ratios (Fig. 8a), (Ca+Mg)/Na ratios (Fig. 8b), and Si+Mg concentrations (Fig. 8c) reflect the absence of Mg-bearing silicates and more albitic plagioclase in the sedimentary aquifer. This suggests no mixing with groundwater from the basalt aquifer occurs.

Groundwater in the local discharge area of the sedimentary aquifer (BHs 13–14; Fig. 2b) is characterized by the highest TDS content (517–537 mg/L) in the system and increased Cl relative to Br due to increased residence times (Cl/Br ratio: 680–740) (Fig. 7a). The source of Cl is possibly minor dissolution of trace residual halite in the sedimentary units. Na/Cl ratios (0.7 to 0.9) are similar to rainfall (Fig. 7b), indicating a loss of Na. This may result from the alteration of kaolinite to montmorillonite (reaction 2). However, Na concentrations are higher than in most other samples so the ongoing dissolution of albite may also be contributing Na, which is reflected in the increased HCO_3 and pH values.

Large variations in groundwater chemistry between sample rounds at the deeper artesian bore (BH 14), compared with the shallower artesian bore (BH 13; Fig. 8b, c) indicates changes in groundwater chemistry in the sedimentary aquifer with depth. A limitation in sampling groundwater from such a long screened interval is that it is unknown exactly from what depths in the sediments the sample has come from. However, the changes in chemistry coupled with the differences in hydraulic heads between the nested bores (Table 3), reflects partly-isolated shallower and deeper flow systems. For the sample round presented in Table 3, the presence of Mg in groundwater from both artesian bores (Figs. 8b, c) represents mixing with more recently-recharged groundwater from the basalt aquifer and therefore a component of flow from the basalt aquifer to the local discharge area. However, TDS content represents more input from the regional flow system dominated by reactions with the sediments and longer flow paths.

Results from additional sample rounds shown for the deeper artesian bore (BH 14; Fig. 8b, c) illustrates other samples which represent greater input from the sedimentary aquifer and less from the basalt aquifer. Therefore, the regional sedimentary aquifer comprises discrete flow paths resulting in variable fluxes from the basalt aquifer feeding different parts of the deeper sedimentary system.

Summary and Conclusions

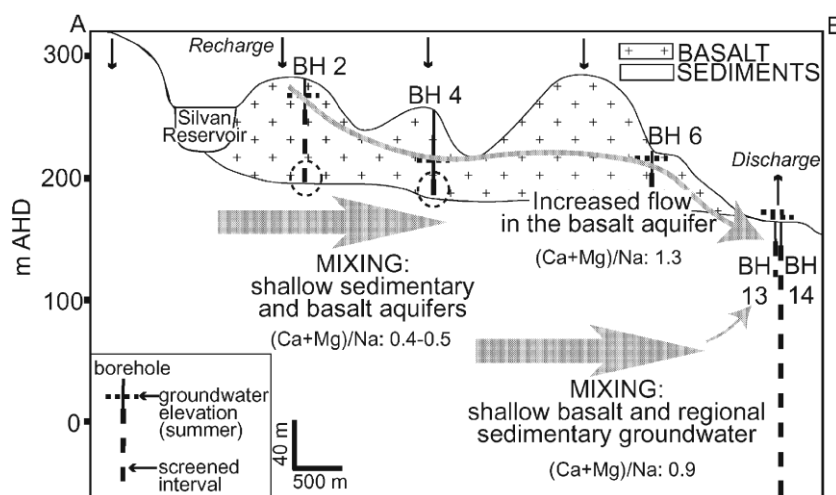
The complications associated with determining groundwater flow paths in fractured rock aquifers are alleviated using major ion chemistry in conjunction with physical hydrogeology. Radon and CFCs were not successful in determining residence times or fracture pathways. However, the use of geochemical tracers has allowed interpretation of relative groundwater residence times within the different aquifers and the extent of inter-aquifer mixing (Fig. 9).

The small seasonal variations in groundwater elevations, major ion and stable isotope geochemistry from most bores, and increasing TDS content down. The hydraulic gradient within the basalt and sedimentary aquifers indicates a system dominated by flow through subhorizontal fractures. The CFC-12 and ^{222}Rn data also indicate the importance of fractures for groundwater flow, especially in the sedimentary aquifer. Vertical flow in this system is limited to local recharge and discharge areas. Increased residence times in the basalt aquifer result in increased TDS content, $(\text{Ca}+\text{Mg})/\text{Na}$ ratios, and $\text{Si}+\text{Mg}$ concentrations due to ongoing mineral dissolution. However, the CFC data indicate that recharge is occurring across the basalt. Increased residence times in the sedimentary aquifer compared with the basalt aquifer are the result of longer flow paths. The ongoing water–rock interaction in the sediments results in the highest TDS contents in the system, and lower $(\text{Ca}+\text{Mg})/\text{Na}$ ratios than in groundwater from the basalt.

The differences in groundwater chemistry between the basalt and sedimentary aquifers allow identification of where mixing has occurred. At the interface between the basalt and sedimentary aquifers, and where groundwater from the sedimentary aquifer enters the basalt aquifer (Fig. 9), the groundwater is more similar to that of the sedimentary aquifer. Groundwater from the basalt aquifer also mixes with sedimentary groundwater in the local discharge area, although the extent of mixing varies with depth.

These results provide clear indications of potential vulnerability of this groundwater resource to surface contamination from agricultural practices, septic systems, minor industry in the area, and to increased salinity from the sedimentary aquifer. To date, agricultural contaminants such as nitrate, have not impacted the shallow groundwater system (0.10 mg/L N). However, increased risk is expected in areas where the water table is shallow, particularly because in thin unsaturated zones rapid recharge occurs. Groundwater resources are more immediately threatened by over-extraction due to irrigation. In the fractured rock aquifers, intense abstraction near the basalt-sedimentary interface will

Fig. 9 Schematic profile of groundwater flow in the Dandenong Ranges sub-catchment shows decreasing hydraulic heads from BH 2–14, interaction between groundwater from the sedimentary and basalt aquifers (e.g. BH 4), and groundwater flow from the basalt aquifer mixing with regional sedimentary groundwater (e.g. BH 13)



increase flow from the deeper groundwater resulting in increased solute load. Over-pumping of either the basalt or sedimentary aquifer could also increase flow from shallower groundwater increasing the vulnerability of groundwater in these aquifers to surface contamination. Since groundwater contributes to surface water, shallow aquifer vulnerability results in increased risk to water resources throughout the catchment. Although specific to the study area, this research can be applied to other fractured-rock systems throughout SE Australia. In hilly terrains, where similar aquifer lithologies, land use and climate will result in similar processes occurring, this research provides valuable management strategies.

Acknowledgements We thank Marlen Yanni for stable isotope analysis, Peter Cook and John Dighton for CFC and radon analysis, and Ian Swane for help with fieldwork. DNRE provided access to bores in the Victorian State Observation Bore Network and the ARC funded this research. The authors also wish to thank the reviewers: P. Olcott, A. Bath, G. Darling and an anonymous reviewer, whose comments improved this paper.

References

- Bierlein FP, Waldron HM, Arne DC (1999) Behaviour of rare earth elements during hydrothermal alteration of meta-turbidites associated with mesothermal gold mineralization in central Victoria, Australia. *J Geochem Explor* 67(1–3):109–125
- Bureau of Meteorology (2000) Average annual rainfall. http://www.bom.gov.au/cgi-bin/climate/cgi_bin_scripts/annual_rnfall.cgi
- Bureau of Meteorology (2002) Data and further information. <http://www.bom.gov.au/climate/how/index.shtml>
- Cecil LD, Green JR (1999) Radon-222. In: Cook P, Herczeg AL (eds) *Environmental Tracers in Hydrology*. Kluwer, Dordrecht, pp 175–194

- Cheng X (1998) Evaluation of the impacts of groundwater abstraction on groundwater flow and solute transport in the Western Port Group Aquifer System, Western Port Basin, Victoria. MSc Thesis, University of Melbourne, Australia
- Clark I, Fritz P (1997) Environmental isotopes in hydrogeology. Lewis, New York
- Cook PG, Solomon DK (1995) Transport of atmospheric trace gases to the water table: implications for groundwater dating with chlorofluorocarbons and krypton 85. *Water Resour Res* 31(2):263–270
- Cook PG, Love AJ, Dighton JC (1999) Inferring ground water flow in fractured rock from dissolved radon. *Ground Water* 37(4): 606–610
- Cook PG, Favreau G, Dighton JC, Tickell S (2003) Determining natural groundwater influx to a tropical river using radon, chlorofluorocarbons and ionic environmental tracers. *J Hydrol* 277:74–88
- Coplen TB (1988) Normalization of oxygen and hydrogen isotope data. *Chem Geol* 72:293–297
- Craig H (1961) Isotopic variations in meteoric waters. *Science* 133:1702–1703
- Cunnold D, Fraser P, Weiss R, Prinn R, Simmonds P, Miller B, Alyea F, Crawford A (1994) Global trends and annual releases of CCl₃F and CCl₂F₂ estimated from ALE/GAGE and other measurements from July 1978 to June 1991. *J Geophys Res* 99(D1):1107–1126
- Cunnold D, Weiss R, Prinn R, Hartley D, Simmonds P, Fraser P, Miller B, Alyea F, Porter L (1997) GAGE/AGAGE measurements indicating reductions in global emissions of CCl₃F and CCl₂F₂ in 1992–1994. *J Geophys Res* 102:1259–1269
- Davis SN, Whittemore DO, Fabryka-Martin J (1998) Uses of chloride/bromide ratios in studies of potable water. *Ground Water* 36(2):338–350
- Davis SN, Cecil LD, Zreda M, Moysey S (2001) Chlorine-36, bromide, and the origin of spring water. *Chem Geol* 179:3–16
- Deer WA, Howie RA, Zussman J (1992) An introduction to the rock-forming minerals, 2nd edn. Wiley, New York
- Department of Natural Resources and Environment (DNRE) Victorian Groundwater database (1999) Groundwater database. <http://www.nre.vic.gov.au/dnre/gmndwtr/g-rdata.htm>
- Domenico PA, Schwartz FW (1998) Physical and chemical hydrology, 2nd edn, Wiley, New York
- Doughty C, Karasaki K (2002) Flow and transport in hierarchically fractured rock. *J Hydrol* 263:1–22
- Drever JI (1997) The geochemistry of natural waters, surface and groundwater environments, 3rd edn. Prentice-Hall, Englewood Cliffs, NJ
- Edmunds WM, Smedley PL (2000) Residence time indicators in groundwater: the East Midlands Triassic sandstone aquifer. *Applied Geochem* 15:737–752
- Edmunds WM, Carrillo-Rivera JJ, Cardona A (2002) Geochemical evolution of groundwater beneath Mexico City. *J Hydrology* 258:1–24
- Edwards AB (1956) The rhyolite-dacite-granodiorite association of the Dandenong Ranges. *Proc RSoc Victoria* 68:111–149
- Faust SD, Aly OM (1981) Chemistry of Natural Waters, Ann Arbor, Ann Arbor, MI
- Folger PF, Poeter E, Wanty RB, Day W, Frishman D (1997) ²²²Rn transport in a fractured crystalline rock aquifer: results from numerical simulations. *J Hydrol* 195:45–77
- Geoscience Victoria's borehole database (1999) Data extracts, Minerals Business Centre, Minerals and Petroleum division, Department of Primary Industries. http://www.dpi.vic.gov.au/web/root/domino/cm_da/nrenmp.nsf/frameset/NRE+Minerals+and+Petroleum?OpenDocument
- Hartley DE, Kindler T, Cunnold DE, Prinn RG (1996) Evaluating chemical transport models: comparison of effects of different CFC-11 emission scenarios. *J Geophys Res* 101:14381–14385
- Healy RW, Cook PG (2002) Using groundwater levels to estimate recharge. *Hydrogeol J* 10:91–109
- Herczeg AL (2001) Can major ion chemistry be used to estimate groundwater residence time in basalt aquifers? In: Cidu R (ed) Water–rock interaction, Balkema, Rotterdam, pp 529–532
- Ho Jeong C (2001) Effect of land use and urbanization on hydrochemistry and contamination of groundwater from Taejon area, Korea. *J Hydrol* 253:194–210
- Huizar AR, Mendez GT, Madrid RR (1998) Patterns of groundwater hydrochemistry in Apan-Tochac sub-basin, Mexico. *Hydrol Sci* 43(5):669–685
- IAEA/WMO (1999) Global Network for isotopes in precipitation. The GNIP Database, Release 3, October 1999, Laboratory code: 9486800, <http://www.iaea.org/programs/ri/gnip/gnipmain.htm>
- Jankowski J, Shekarforoush S, Acworth RI (1998) Reverse ionexchange in a deeply weathered porphyritic dacite fractured aquifer system, Yass, New South Wales, Australia. In: Arehart GB, Hulston JR (eds) Water–rock interaction, Balkema, Rotterdam, pp 243–246
- Langmuir D (1997) Aqueous environmental geochemistry, McConnin RA (ed), Prentice-Hall, Englewood Cliffs, NJ
- Lee ES, Krothe NC (2001) A four-component mixing model for water in a karst terrain in south-central Indiana, USA. Using solute concentration and stable isotopes as tracers. *Chem Geol* 179:129–143
- Leonard J (1992) Port Phillip region groundwater resources: future use and management. Department of Water Resources, Victoria
- Marsden MAH (1988) Upper Devonian: Carboniferous. In: Douglas JG, Ferguson JA (eds) Geology of Victoria, Victn. Div. Geol. Soc. Aust., Melbourne, pp 147–194
- Martin CE, McCulloch MT (1999) Nd-Sr isotopic and trace element geochemistry of river sediments and soils in a fertilized catchment, New South Wales, Australia. *Geochim Cosmochim Acta* 63(2):287–305
- Njitchoua R, Dever L, Fontes JCh, Naah E (1997) Geochemistry, origin and recharge mechanisms of groundwaters from the Garoua Sandstone aquifer, northern Cameroon. *J Hydrol* 190: 123–140
- Parkhurst DL, Appelo CAJ (1999) User's guide to PHREEQC (version 2): a computer program for speciation, batch-reaction, one-dimensional transport, and inverse geochemical calculations. US Geological Survey Water-Resources Investigations Report 99–4259, US Geol Surv, Reston, Va.
- Plummer LN, Busenberg E (1999) Chlorofluorocarbons. In: Cook PG, Herczeg AL (eds) Environmental tracers in subsurface hydrology, Kluwer, Dordrecht, pp 441–478
- Port Phillip Catchment and Land Protection (1999) Yarra Catchment Action Plan. Port Phillip and Westernport Catchment Management Authority, Frankston, Victoria
- Price RC, Gray CM, Nicholls IA, Day A (1988) Cainozoic volcanic rocks. In: Douglas JG, Ferguson JA (eds) Geology of Victoria, Victn. Div. Geol. Soc. Aust., Melbourne, pp 439–451
- Puls RW, Barcelona MJ (1996) Low-flow (minimal drawdown) ground-water sampling procedures. EPA Ground Water Issue EPA/540/S-95/504, US EPA, Washington, DC

- Sanders RG (1992) Silurian and Lower Devonian. In: Peck WA, Neilson JL, Olds RJ, Seddon KD (eds) Engineering geology of Melbourne. Balkema, Rotterdam, pp 75–94
- Shapiro AM (2002) Cautions and suggestions for geochemical sampling in fractured rock. *Ground Water Monitor Remed* 22(3):151
- Shugg A (1996) Hydrogeology of the Dandenong Ranges fractured rock aquifers and the comparison with similar aquifers in Victoria. MSc Thesis, Sydney University of Technology, Sydney, Australia
- Shugg A, O'Rourke M (1995) Groundwater in the Yarra Basin. Technical document, YarraCare, Victoria
- Stumm W, Morgan JJ (1996) *Aquatic Chemistry: chemical equilibria and rates in natural waters*, 3rd edn. Wiley, New York
- Swanson SK, Bahr JM, Schwar MT, Potter KW (2001) Two-way cluster analysis of geochemical data to constrain spring source waters. *Chem Geol* 179:73–91
- Tweed SO (2003) Groundwater chemistry in the Dandeong Ranges sub-catchment: application to aquifer vulnerability in the greater Yarra catchment, Victoria, Australia. PhD Thesis, University of Melbourne, Melbourne, Australia
- Uliana MM, Sharp Jr JM (2001) Tracing regional flow paths to major springs in Trans-Pecos Texas using geochemical data and geochemical models. *Chem Geol* 179:53–72
- Vandenberg AHM (1988) Silurian: Middle Devonian. In: Douglas JG, Ferguson JA (eds) *Geology of Victoria*, Victn. Div. Geol. Soc. Aust., Melbourne, pp 103–146
- Victorian Resources Online (2003) Groundwater basins map database. <http://www.nre.vic.gov.au/web/root/Domino/vro/maps.nsf/pages/Victoria-NaturalResources-Water-Groundwater-grwaterbasins?Opendocument>
- Vengosh A, Hendry MJ (2001) Chloride-bromide-delta B-11 systematics of a thick clay-rich aquitard system. *Water Resour Res* 37(5):1437–1444
- Weaver TR, Frape SK, Cherry JA (1995) Recent cross-formational fluid-flow and mixing in the shallow Michigan basin. *Geol Soc Am Bull* 107(6):697–707